GALAXY SIMULATIONS OF VISUAL BINARY STARS

P. Nurmi[1,2]

[1]Royal Observatory of Belgium, Av. Circulaire, 3, 1180 Brussels, Belgium
[2]Tuorla Observatory, Väisäläntie 20, 21500 Piikkiö, Finland

ABSTRACT

The simulated binary star catalogue that represents the full sky distribution of stars down to $m_G = 20$ mag is constructed. The catalogue is based on the Galaxy model and the fundamental physical parameter distributions of the stars and binaries. Instead of using observed luminosity functions, we use stellar and binary evolution routines to simulate stellar and binary evolution in different Galaxy populations and to calculate the physical properties of the stars in a given galactic direction. The model has been extensively tested so that the number and the colour distributions of the stars agree well with the observations. The simulated catalogue is analyzed for observational properties of binary stars considering the observational capabilities of Gaia in eight different galactic samples. Detailed predictions for different types of visual binaries are given.

Key words: Gaia; Galaxy simulations; Visual binaries.

1. INTRODUCTION

The artificial binary star catalogue that we have created has statistically similar properties to the expected final output catalogue of Gaia. The catalogue represents the overall distribution of stars in the sky down to Gaia magnitude $m_G = 20$. This limit is the expected detection level for the GAIA. The Galaxy model used in the simulations is tested and optimized so that the predicted calculations of the simulations are compatible with the observed stellar counts in different regions of the sky. One example of the test simulations is shown in Figure 1, where the calculated $B - V$-colour histograms are compared with the observations using the data from Hall et al. (1996) in six different galactic directions. In general, the agreement between the simulations and the observations is fairly good.

2. THE METHOD

The construction of the artificial Galaxy is started by choosing the primary star from the Initial Mass Function (IMF). The secondary mass is calculated using the mass-ratio distribution that is based on the Duquennoy & Mayor (1991) distribution, but we have included an additional peak close to equal masses. The existence of the second peak close to equal masses is supported by Halbwachs et al. (2003). After choosing the masses of the components (or individual stars) the stars and binary systems are evolved according to their ages and metallicities using the stellar evolution codes. A uniform distribution of ages is assumed and also the star formation rate is assumed to be constant.

The IMF used in the calculations consists of two parts:

$$dn/dm \propto m^{-\alpha}, \tag{1}$$

where α is 1.3 for $m < 1M_{\odot}$ and α is 2.7 for $m > 1M_{\odot}$. In the simulations by Robin et al. (2003), they found that the observed luminosity function requires a notably lower value of the slope for the low mass stars than that of Kroupa (2002). Robin et al. (2003) found that $\alpha = 1.6$ for $m < 1M_{\odot}$. In our model an even smaller value gives a better fit with the observations when the simulated luminosity function is compared with the observations. The lower limit of the stellar masses is $0.08M_{\odot}$, hence brown dwarfs are not included in the simulations. The upper limit of the mass for the individual stars is $100M_{\odot}$. The IMF is the same for all the Galaxy populations.

Since we start our calculation from the IMF, we have to evolve the stars to derive the present-day masses and luminosities. The stellar evolution code that we have used is based on the stellar evolutionary algorithms by Hurley et al. (2000) and the binary evolution is based on the Hurley et al. (2002).

The number of stars in a given direction is calculated using the stellar density distribution functions. The Galaxy model used in the simulations is the classical three component Galaxy model that includes the disc, the thick disc and the halo (Gilmore & Reid 1983; Robin et al. 2003). The standard double-exponential density law distributions are adopted for the disc components and the

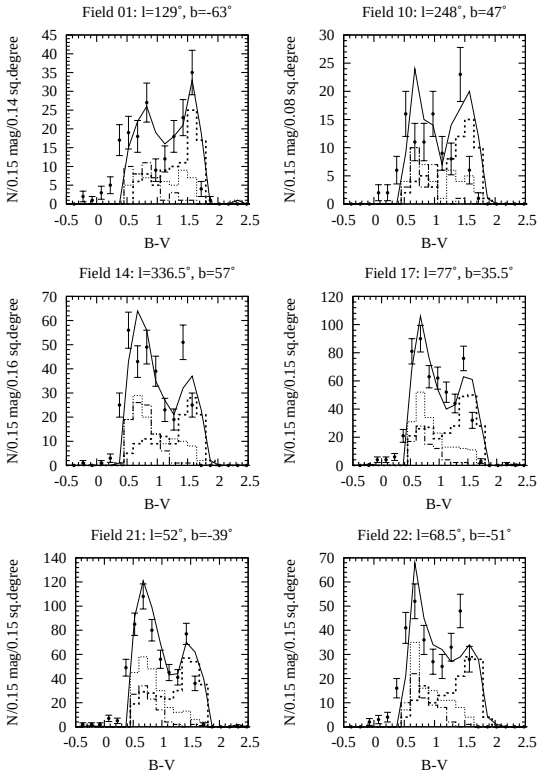

Figure 1. Comparison of the observed (DMS data taken from Hall et al. 1996) and simulated $B-V$ number distributions in six different galactic directions. The observed numbers are shown as points together with their Poisson error bars. The solid line gives the total distribution. Thick dashed line denotes the disc component, thin dashed line is for the halo component and the dot-dashed line is for the thick disc component.

stars in the halo have a power-law distribution. The nominal binary frequency of 0.75 is adopted for all the stars in the Galaxy. The Galaxy model parameters that are obtained after extensive tests with the observed data are listed in Table 1.

To study the variations of the number statistics in different regions of the Galaxy we have chosen random fields in eight different galactic directions (see Figure 2). The number of fields in different directions varies in every sample, but we aimed to have at least $\sim 10^5$ stars in every sample. The details of the number of stars, the number of fields and the total coverage of the samples are given in Table 2.

3. GENERAL PROPERTIES

At first we look at general properties of the distributions of the main observables: magnitude difference Δm_G and colour $V-I$-distribution (Figures 3 and 4). These distributions are from the sample b(2). The magnitude difference distribution has a peak close to equal magnitudes and a flat plateau between 1 and 6 magnitudes. After this limit the number of binaries diminishes gradually. In

Table 1. Summary of the parameters used in the Galaxy model. The Sun is located at $Z_0 = 27.5$ pc and $R_0 = 8.5$ kpc. The scale height is h_z and the scale length is h_l. The halo parameters, ϵ and n, are the axis ratio and the power law index of the density distribution, considerably.

Component	Age [10^6yr]	Metallicity(Z)	
Disc	0.5–10 000	0.007–0.03	
Thick Disc	10 000–12 000	0.0017–0.007	
Halo	10 000–14 000	0.0001–0.001	
Component	h_l [pc]	h_z [pc]	Norm.
Disk	2500	$\propto M_V$	1
Thick Disc	3100	850	0.065
	ϵ	n	
Halo	0.75	-2.44	0.001

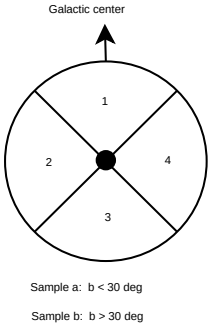

Figure 2. Galaxy simulation samples used in the statistical analysis of the catalogue data.

all the directions the common feature is the double peak structure in the colour distribution that follows from the disc and the halo distributions. The red stars are generally G or F-type dwarfs from the disc and the blue stars are early type stars in the thick disc and the halo.

It is interesting to estimate how the combined (generally observed) colour differs from the colour of the primary. As can be seen in Figure 4 the system colour is very close to the colour of the primary that normally dominates the colour of the system. We estimate that the difference is generally < 0.2 mag. Another interesting comparison is to plot the magnitude difference Δm against the mass ratio Q (Figure 5). The mass ratio can exceed one, since the primary has been defined to be always the brighter component from the two, but not necessarily more massive. The two values are correlated, but variations are very large. Hence, it is apparent that the magnitude difference alone is not very good indicator for the mass-ratio. For faint visual binaries $m_G > 18$ mag to which we don't have spectral information or colour information, it may be very difficult to determine the mass ratio.

Table 2. The general number statistics of the simulations for all stars in the Galaxy ($m_G \leq 20$) mag. The Galaxy has been divided into 8 different regions (see Figure 2).

Sample	Area [sq.deg.]	N(sample)	N(Galaxy)	N(Disc)	N(Thick disc)	N(Halo)	Fraction
a(1)	3	318 143	5.47×10^8	4.51×10^8	8.69×10^7	9.16×10^6	0.55
a(2)	30	905 274	1.56×10^8	1.30×10^8	2.34×10^7	2.10×10^6	0.16
a(3)	50	713 789	7.36×10^7	6.42×10^7	8.55×10^6	8.38×10^5	0.073
a(4)	30	944 229	1.62×10^8	1.35×10^8	2.54×10^7	2.12×10^6	0.16
b(1)	150	709 037	2.44×10^7	1.18×10^7	8.77×10^6	3.84×10^6	0.024
b(2)	200	570 022	1.47×10^7	8.24×10^6	4.49×10^6	1.97×10^6	0.015
b(3)	300	599 413	1.03×10^7	6.19×10^6	2.85×10^6	1.26×10^6	0.010
b(4)	200	569 046	1.47×10^7	8.17×10^6	4.50×10^6	2.00×10^6	0.015
Sum	963	5 328 953	1.0×10^9	8.14×10^8	1.65×10^8	2.26×10^7	1.0

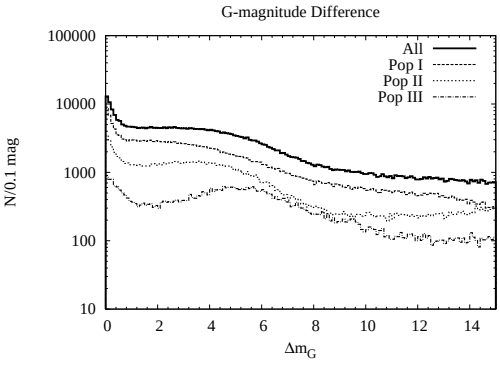

Figure 3. Magnitude difference distribution of the three galactic components for the sample b(2).

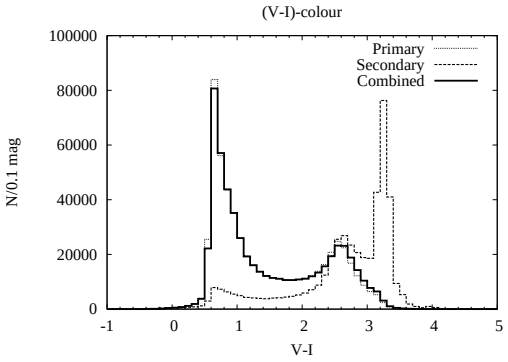

Figure 4. V-I-colour distribution of the sample b(2).

The total number of systems in different samples and galactic populations is shown in Table 2. There are $\sim 6{\times}10^6$ stars in the samples and the total areal coverage is 963 square degrees. The coverage is $\sim$ 2.3% of all the stars in the sky down to $m_G = 20$ mag. The total number of systems that Gaia is able to observe in the Galaxy is $\approx 10^9$ from which $\sim$ 50% are in the sample that points towards the galactic center. Only $\sim$ 6% of the stars are in the high galactic latitudes with $b >30°$.

There is a wide variety of different types of binaries in the Galaxy that Gaia can observe. The stellar types of the binary components have been divided into 5 different groups: main-sequence stars ($M < 0.7M_\odot$ and $M \geq 0.7M_\odot$), evolved stars (including giants and supergiants), white dwarfs and compact objects (neutron stars and black holes). In Table 3 the total numbers of 20 different types of binaries are shown. The secondary type is given in the horizontal direction and the vertical direction gives the primary stellar type. Most of these systems are not observable as binaries, since they are unresolved or the secondary component is too faint to be observed. The expected number of resolved systems is given in parenthesis below the total number of systems existing in the Galaxy. The detailed calculation of what kind of binaries Gaia will evetually observe is a very difficult task that requires the combination of photometric, astrometric and spectral information. Hence, here we concentrate only on the visual binaries.

To have some idea about the number of exotic binary systems we have calculated how many contact binaries, where one of the components fills its Roche lobe, our list contains. All together there are 2.9×10^5 interacting binaries from which roughly half are systems with a white dwarf companion. There are only 5600 interacting binaries, where one of the binary components is a neutron star or a black hole.

4. VISUAL BINARIES

To estimate the number of visual binaries the artificial binary catalogue is analyzed with three different observability criteria. The data is divided into 8 different spectral type regions based on the effective temperatures of the stars (Table 4). The number of true single stars is shown in the first column. In the second and the third column we show the number of visual binaries with two different observability criterias: ($m_G(1,2) \leq 20$, $\theta \geq 88.4$ mas and $\Delta m \leq 4$) and ($m_G(1) \leq 20$,

Table 3. The primary (vertical) and the secondary (horizontal) stellar types of the binary stars in the Galaxy ($m_G(system) \leq 20$ mag). The numbers of visual resolved binaries are given in parenthesis (see also Section 4).

	MS: $M < 0.7M_\odot$	MS: $M \geq 0.7M_\odot$	Evolved	White Dwarf	Compact
MS: $M < 0.7M_\odot$	9.33×10^7	0	0	7.87×10^6	39 920
	(3.29×10^6)	(-)	(-)	(-)	(-)
MS: $M \geq 0.7M_\odot$	3.46×10^8	1.50×10^8	4.25×10^5	7.36×10^7	1.39×10^6
	(7.64×10^6)	(5.54×10^6)	(-)	(-)	(-)
Evolved	5.77×10^7	2.49×10^7	2.66×10^6	2.26×10^7	3.34×10^5
	(4.61×10^5)	(7.74×10^5)	(9.59×10^4)	(-)	(-)
White Dwarf	20 730	0	0	30 560	1100
	(1014)	(-)	(-)	(43)	(-)

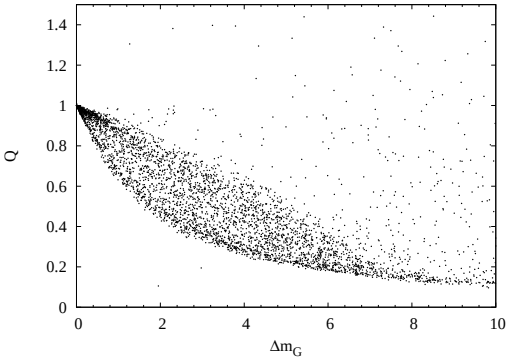

Figure 5. The mass ratio Q plotted as a function of magnitude difference Δm_G for the sample b(2).

$m_G(2) \leq 24$, $88.4 \leq \theta \leq 1250$ mas and $\Delta m \leq 8$ mag), where θ is the mutual angular separation. In addition, if the system belongs to the first group it is not calculated again in the second case. The first limit is for the easy detection and the second limit has been chosen to represent the ultimate limits that can be achieved by combining the data from all the transits to one combined image in the astrometric AF11 field of view (see Nurmi 2004).

Table 4. The expected number of systems that are observable by Gaia.

	Single	Visual	Visual 2	Unresolved
O	37 805	198	26	1.14×10^5
B	4.73×10^6	3.09×10^5	2.19×10^5	1.45×10^7
A	3.73×10^6	1.88×10^5	1.54×10^5	1.16×10^7
F	7.72×10^7	2.45×10^6	3.58×10^6	2.56×10^8
G	1.07×10^8	2.51×10^6	5.08×10^6	3.66×10^8
K	1.87×10^7	6.91×10^5	1.22×10^6	6.43×10^7
M	1.07×10^7	5.87×10^5	8.20×10^5	3.82×10^7
BD	28 610	782	1590	71 680
Sum	2.22×10^8	6.73×10^6	1.11×10^7	7.50×10^8

ACKNOWLEDGMENTS

The author wants to acknowledge the Belgian Science Policy and ESA-ESTEC for the financial support through the PRODEX-grant 'Double stars: From Hipparcos to Gaia' with contract number 14847/00/NL/SFe(IC). The author also thanks Dr. Henri Boffin and Dr. Staffan Söderhjelm for all the helpful discussions and ideas related to this work.

REFERENCES

Duquennoy, A., Mayor, M., 1991, A&A, 248, 485

Gilmore, G. & Reid, N., 1983, MNRAS, 202, 1025

Halbwachs, J. L., Mayor, M., Udry, S., & Arenou, F., 2003, A&A, 397, 159

Hall, P. B., Osmer, P. S., Green, R. F., et al., 1996, ApJS, 104, 185

Hurley, J. R., Pols, O. R., Tout, C. A., 2000, MNRAS, 315, 543

Hurley, J.R., Tout, C.A., Pols, O.R. 2002, MNRAS, 329, 897

Kroupa, P., 2002, Science, 295, 82

Nurmi, P., 2004, Astrophysics and Space Science, accepted for publication

Robin, A. C., Reylé, C., Derrière, S., Picaud, S., 2003, A&A 409, 523